Electrochimica Acta 55 (2010) 1401–1406

Contents lists available at ScienceDirect

Electrochimica Acta

journal homepage: www.elsevier.com/locate/electacta

Ionic conductivity and interfacial properties of nanochitin-incorporated polyethylene oxide–$LiN(C_2F_5SO_2)_2$ polymer electrolytes

N. Angulakshmi[a], T. Prem Kumar[a], Sabu Thomas[b], A. Manuel Stephan[a,*]

[a] Electrochemical Power Systems Division, Central Electrochemical Research Institute, Karaikudi 630006, India
[b] School of Chemical Sciences, Mahatma Gandhi University, Kottayam 686560, India

ARTICLE INFO

Article history:
Received 13 October 2008
Received in revised form 16 March 2009
Accepted 21 April 2009
Available online 3 May 2009

Keywords:
Nanocomposites
Chitin
Interfacial properties
Ionic conductivity
Cycling profile

ABSTRACT

Nanocomposite polymer electrolytes (NCPE) composed of poly(ethylene oxide) and nanochitin for different concentrations of $LiN(C_2F_5SO_2)_2$ (LiBETI) were prepared by a completely dry, solvent-free procedure using a hot press. The thermal stability of NCPE membranes was investigated by DSC and TG-DTA. The membranes were subjected to SEM, ionic conductivity and FTIR analysis. Li/NCPE/Li symmetric cells were assembled and the variation of interfacial resistance as a function of time was also measured. The surface chemistry of lithium electrodes in contact with NCPE revealed the formation of Li–O–C and LiN compounds. $LiFePO_4$/NCPE/Li cell was assembled and the cycling profile showed a well-defined and reproducible shape of the voltage curves thus indicating a good cycling behavior of the cell at 60 °C.

1. Introduction

Although lithium batteries acquired a leading position in the consumer market right from portable devices to hybrid electric vehicles considering the evolution and their associated energy and power demands, new and improved battery components are required [1–3]. In order to achieve this goal various strategies have been employed. Among this, the replacement of conventional liquid electrolyte structure by an advanced polymer electrolyte configuration has been identified as most relevant procedure when safety and reliability are concerned [4,5]. Also the liquid electrolytes with organic solvents are flammable and easy to ignite upon exposure to high temperatures. This non-aqueous electrolyte can be replaced by a polymer membrane which acts as both electrolyte and separator between electrodes.

Among the polymer hosts examined poly(ethylene oxide) (PEO)-based electrolytes have been widely studied due to its ability to form complexes with a variety of lithium salts [6]. The transport of Li^+ ions in PEO-based electrolytes is related to the local relaxation and segmental motion of PEO chains [7]. However these electrolytes exhibit very low ionic conductivity (order of 10^{-7} S cm^{-1}) at ambient and sub-ambient temperatures [8,9]. Although the incorporation of low molecular weight plasticizers offers high ionic conductivity it adversely deteriorates the mechanical strength of the polymer membranes [10–12]. One of the most successful methods of electrolyte modification is the use of inorganic filler [13–16]. This leads to an increase not only in ionic conductivity [16] but also improves its thermal stability and mechanical strength [17].

Numerous attempts have been made with the incorporation of nanosized oxide fillers such as TiO_2, SiO_2, Al_2O_3, ZrO_2, etc., in the polymer matrix [9]. In the present study nanochitin has been incorporated as filler for the first time. Chitin, a biopolymer has low toxicity, biodegradable, antibacterial, and also possesses gel-forming properties and also finds applications in biosensors [18]. The molecular structure of chitin is depicted in Fig. 1. Recent study reveals [19–21] that chitin forms a three-dimensional network among the chitin whiskers and this particular aspect has prompted us to explore the possibility of employing chitin incorporated PEO–LiTFSI systems for battery applications.

2. Experimental

2.1. Synthesis of nanochitin

The chitin precursor purchased from local sources in India was boiled and stirred with a 5% aqueous solution of KOH for 6 h in order to remove most of the proteins. Subsequently, it was washed with distilled water and dried. This process was repeated three times. The sample was then bleached with 17 g of NaCl in 1 L of water containing 0.3 M sodium acetate buffer for 6 h at 80 °C. The bleaching solution was changed every 2 h. The chitin suspension was then kept in 5% KOH for 72 h to remove any residual protein, centrifuged

* Corresponding author. Fax: +91 4565 227779.
E-mail address: arulmanuel@gmail.com (A. Manuel Stephan).

0013-4686/$ – see front matter © 2009 Elsevier Ltd. All rights reserved.
doi:10.1016/j.electacta.2009.04.055

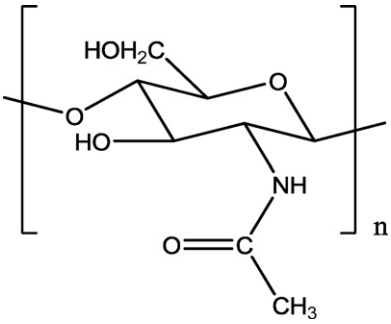

Fig. 1. Molecular structure of chitin poly(N-acetyl-β-D glucosamine).

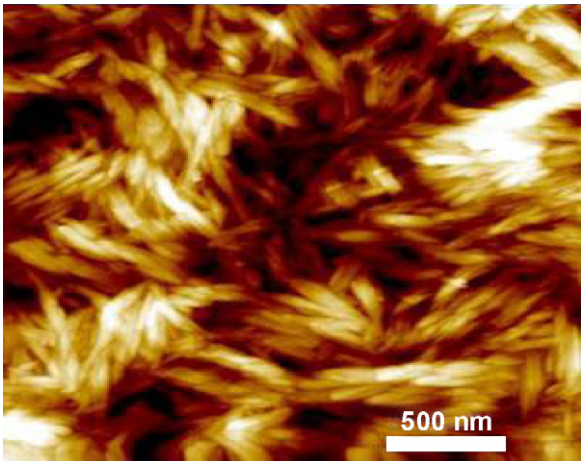

Fig. 2. AFM image of nanochitin.

at 3000 rpm/min for 20 min, and hydrolyzed with 3N HCl under stirring for 1.5 h. After hydrolysis, the suspension was transferred to a dialysis bag and dialyzed for 24 h until its pH reached a value of 6. The pH of the suspension was adjusted to 3.5 with HCl. The dispersed whiskers were treated ultrasonically and were filtered to remove residual aggregates. The prepared nanochitin particles were of size between 400 and 500 nm of length and diameter of 1 nm and its AFM picture is displayed in Fig. 2. The prepared nanochitin was preserved in a refrigerator with sodium azoture as a protectant against microorganisms.

2.2. Preparation of nanocomposite polymer electrolytes

PEO (M_w = 200,000, Aldrich, USA) and $LiN(C_2F_5SO_2)_2$ (Merck) were dried under vacuum for 2 days at 80 and 70 °C, respectively. Nanochitin was also dried under vacuum at 50 °C for 5 days before use. Nanocomposite electrolytes were prepared by dispersing chitin in PEO–$LiN(C_2F_5SO_2)_2$ compositions (Table 1), was hot-pressed into films, as described elsewhere [22,23]. The nanocomposite electrolyte films had an average thickness of 30–50 μm. This procedure yielded homogenous and mechanically strong membranes, which were dried under vacuum at 50 °C for 24 h for further characterization.

Table 1
Compositions of polymer, chitin and LiTFSI.

Sample	Polymer (wt.%)	Chitin (wt.%)	LiTFSI (wt.%)
S1	95	0	5
S2	94	5	1
S3	93	5	2
S4	92	5	3
S5	90	5	5
S6	88	2	10
S7	86	4	10
S8	82	8	10
S9	74	16	10

2.3. Characterization of nanocomposite polymer electrolytes

The ionic conductivity of the membranes sandwiched between two stainless steel blocking electrodes (1 cm^2 diameter) was measured using an electrochemical impedance analyzer (IM6-Bio Analytical Systems) in the 50 mHz to 100 kHz frequency range at various temperatures (0, 15, 30, 40, 50, 60, 70 and 80 °C). Symmetric non-blocking cells of the type Li/CPE/Li were assembled for compatibility studies and were investigated by studying the time-dependence of the impedance of the systems under open circuit at 80 °C.

Morphological examination of the films was made by a scanning electron microscope (FE-SEM, S-4700, Hitachi) under a vacuum condition (10^{-1} Pa) after sputtering gold on one side of the films. Differential scanning calorimetry measurements were performed at a rate of 10 °C min^{-1} between 20 and 250 °C while TG-DTA in the temperature range 20–300 °C. The lithium/polymer electrolyte interface was analyzed using FTIR (Thermo NICOLET Corporation, Nexus Model-670) by single internal reflection (SIR) mode [24]. The infra-red spectra were obtained at ambient temperature with an 8 cm^{-1} resolution.

3. Results and discussion

3.1. Thermal analysis

Fig. 3(a and b) depicts the DSC curves of PEO + $LiN(C_2F_5SO_2)_2$ and PEO + $LiN(C_2F_5SO_2)_2$ + nanochitin, respectively. The melting endotherm of PEO + $LiN(C_2F_5SO_2)_2$ (66 °C) gets broadened and the melting temperature gets reduced as the concentrations of nanochitin was increased. Further the addition of nanochitin, decreases the crystallinity of PEO as evident from the decrease in magnitude of ΔH_m and shifting of melting point to lower temperature. A similar observation has been reported by Fan and Maier [25] where the authors reported the thermal behavior of PEO–succinonitrile-based electrolytes. In order to evaluate the stability of polymer electrolytes the thermogravimetric analysis of the NCPE was performed in air. The TG-DTA traces of PEO + $LiN(C_2F_5SO_2)_2$ and PEO + $LiN(C_2F_5SO_2)_2$ + nanochitin membranes are displayed in Fig. 4(a) and (b), respectively. A weight loss of about 2% was observed about 50 °C and is attributed to the release of water absorbed at the time of loading the sample [26,27]. A very good thermal stability was observed up to 170 °C which indi-

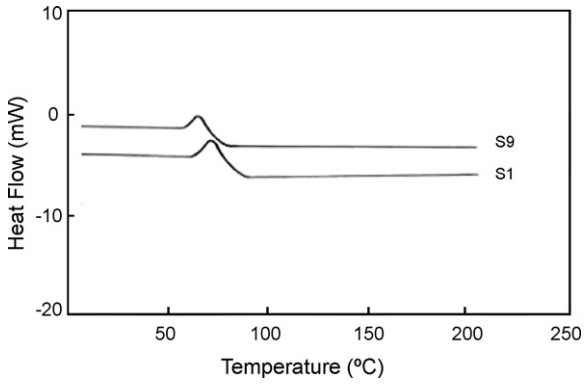

Fig. 3. DSC traces of sample (S1) and (S9).

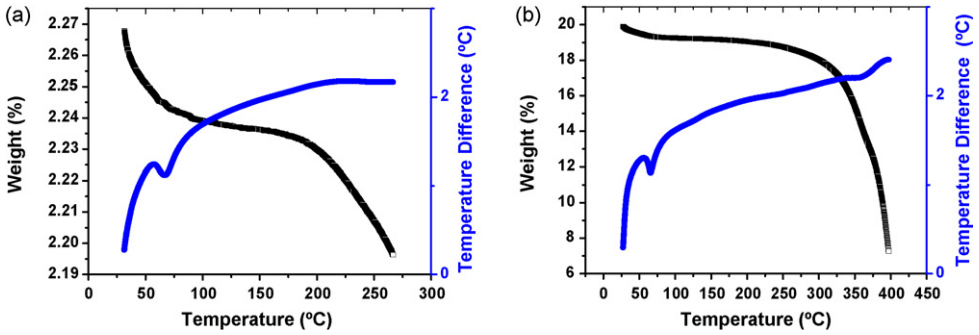

Fig. 4. TG-DTA traces of (a) PEO + LiTFSI and (b) PEO + LiTFSI + chitin.

cates that no deterioration was induced by the thermal steps of the hot-pressing process [23].

3.2. SEM analysis

Generally the morphology of the membranes can be tailored by the incorporation ionic salts and/or fillers [28–30]. The surface morphology of PEO + chitin and PEO + chitin + LiTFSI membranes are displayed in Fig. 5(a) and (b), respectively. The membrane which possesses PEO + chitin shows a flaky morphology. On the other hand, chitin particles are uniformly distributed throughout the matrix of the polymer and are attributed to the formation of a rigid chitin–chitin network [19–21]. A similar observation has been reported by Dufresne and co-workers where the authors studied the morphological behavior of chitin incorporated natural rubber nanocomposites [19–21].

3.3. FTIR analysis

FTIR has been identified as a powerful tool to study the complexation between salts and polymers as it is sensitive to molecular and structural changes in the polymer systems.

The FTIR spectra of PEO, chitin, PEO + $LiN(C_2F_5SO_2)_2$ and PEO + $LiN(C_2F_5SO_2)_2$ + chitin are displayed in Fig. 6(a–d), respectively. The band that appears at 2886 cm^{-1} is attributed to an asymmetric stretching mode and the peak at 1967 cm^{-1} to a symmetric mode. The peaks at 1466, 1103, 956 and 841 cm^{-1} are assigned to $-CH_2-$ scissoring, –C–O–C– stretching, $-CH_2$ twisting and $-CH_2-$ wagging modes, respectively. Also, PEO exhibits –C–H stretching (between 2800 and 2935 cm^{-1}) asymmetric stretching (1950–1970 cm^{-1}), asymmetric bending (1450 cm^{-1}), CH_2 scissoring (1465–1485 cm^{-1}), C–O–O stretching (1250–950 cm^{-1}), $-CH_2-$ twisting (991 cm^{-1}) and $-CH_2-$ wagging (842 cm^{-1}) [31–33]. The spectra of α-chitin (Fig. 6b) is typical of (polysaccharides), and because of the high crystallinity of the samples they show a series of very sharp absorption bands. The amide I band is split in to two at 1659 and 1626 cm^{-1}. The band at 1656 cm^{-1} commonly assigned to stretching of the C=O group hydrogen bonded to N–H of the neighboring intra-sheet chain of (polyamides) and proteins [31]. The band at 1626 cm^{-1} is attributed to a specific hydrogen bond of C=O in the hydroxyl methyl group of the next chitin residue of the same chain [18]. The strongest peak, the C–O–C at 1104 cm^{-1} in pure PEO is shifted to 1106 cm^{-1} in the complex (Fig. 6c). Similarly the C–H stretching band centered around 2900 cm^{-1} is quite sensitive to the lithium salt complexation like the bending and rocking modes around 1460 and 850 cm^{-1}, respectively [31–34]. In each case the bands are split into two or more components, becoming more resolved and the complex formation was identified. On the other hand in Fig. 6(d) the intensity of the peaks at 1659 and 1629 cm^{-1} which corresponds to amide I band of chitin, has been

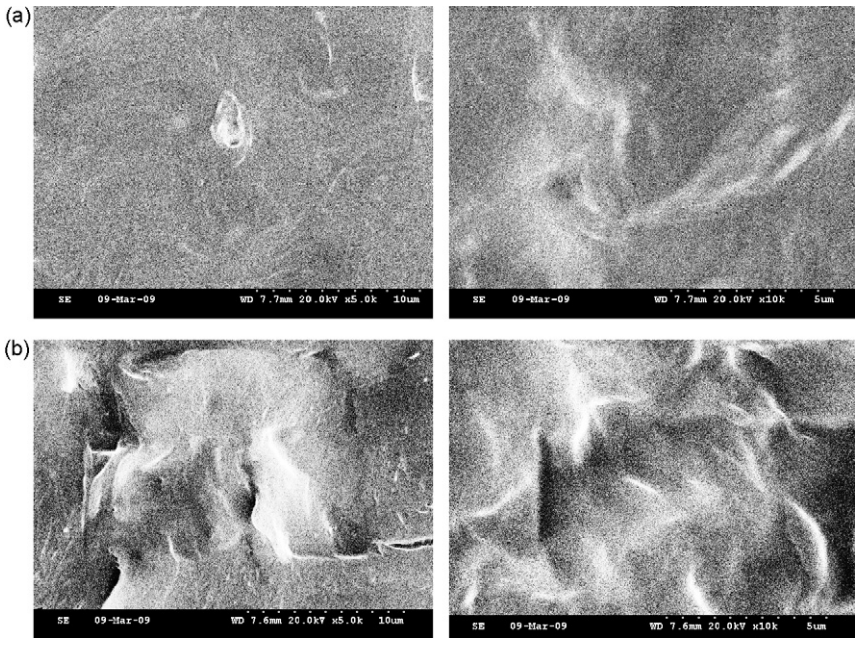

Fig. 5. SEM images of (a) PEO + LiBETI and (b) PBO + LiBETI + chitin.

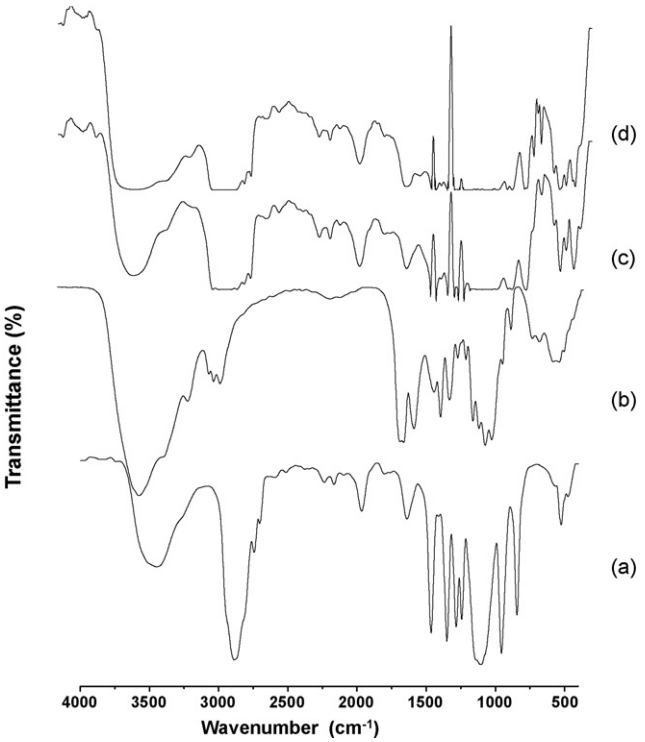

Fig. 6. FTIR spectra of (a) PEO, (b) chitin, (c) PEO + chitin, and (d) PEO + chitin + LiTFSI.

broadened and reduced intensity reduced further substantiates the complex formation in the PEO + chitin + LiBETI systems.

3.4. Ionic conductivity

The variation of ionic conductivity as a function of temperature is depicted in Fig. 7(a) and (b) for different concentrations of chitin and lithium salt, respectively. It can be seen from Fig. 7(a) that the ionic conductivity increases with the increase of temperature and also increases with the increase of lithium salt, LiBETI up to (3 wt.%, sample S4). After that, the ionic conductivity gets reduced with further increase of lithium salt concentration (sample S5). A similar trend has been observed (Fig. 7(b)) when the concentration of chitin was increased above 8 wt.% (sample S8). All the curves (Fig. 6(a)) show a slow and continuous change in the slope up to around 60 °C, beyond which there a remarkable change in slope, reflecting the well-known transition from the crystalline to the amorphous phase of PEO. This transition contributes to an increase in ionic

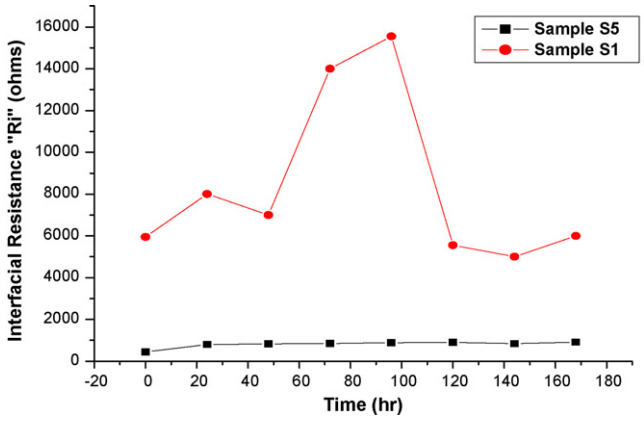

Fig. 8. Variation of interfacial resistance (Ri) as a function of time for the symmetric cell Li/NCPE/Li at 80 °C.

conductivity. These results are in accordance with those reported on PEO-based polymer electrolytes with SiO_2–lithium imide anion systems [35,36]. Fig. 7(b) clearly illustrates that incorporation of nanochitin fillers enhances the ionic conductivity up to one order magnitude.

According to Wieckzorek et al. [37], the Lewis base reactions between the filler surface and the PEO segments may induce structural modifications in the polymer matrix. The Lewis acid character of the added ceramics (γ-Al_2O_3) would compete with the Lewis acid character of the of the lithium cations for the formation of complexes with the PEO chains. In the present study, chitin would act as cross-linking centers for the PEO segments, which lowers the polymer chain reorganization tendency, thus promoting an overall stiffness to the structure. However, the resulting structure provides Li^+-conducting pathways at the filler surface and enhances ionic transport [38].

3.5. Interfacial properties

The interfacial properties of lithium metal anodes in contact with the electrolyte are critical in practical applications. Fig. 8 shows the variation of the interfacial resistance as a function of time for the symmetric cells Li/NCPE/Li at 80 °C. The interfacial resistance values increases and decreases in an irregular manner. However, the values of the interfacial resistance of chitin-added samples are substantially lower than that of the filler-free sample. Furthermore, the interfacial resistance remained stable over long periods of storage (240 h). The considerable decrease in the interfacial resistance of chitin-added membranes may be attributed to the formation of a

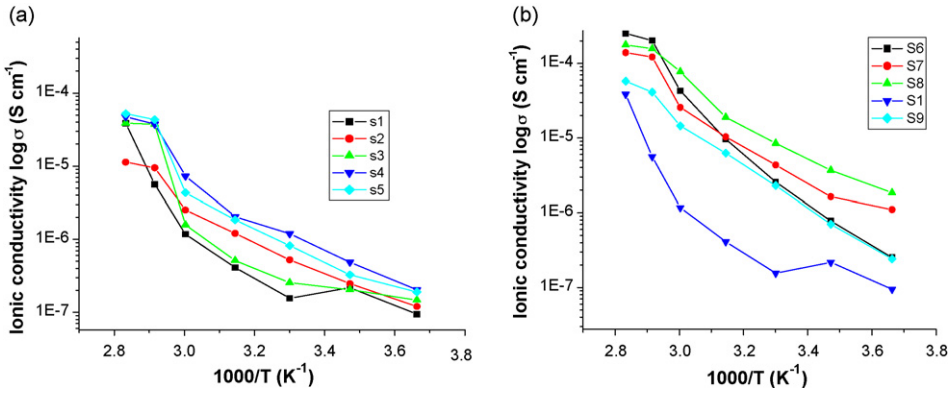

Fig. 7. Ionic conductivity as a function of temperature for the various (a) lithium salt concentrations and (b) chitin concentrations.

chitin–chitin three-dimensional network [19–21] which may minimize area of lithium metal anode exposed to polymer and thus reduce the passivation process.

Numerous attempts have been made on the charge–discharge characteristics of lithium anode [39,40]. Only a few studies focus on the interfacial properties of lithium and lithiated-carbon electrodes in contact with solid polymer electrolytes. The solid polymer electrolyte–lithium interface plays a vital role in the electrochemical behavior of the lithium-polymer cells [41]. Infra-red spectroscopic measurements provide information on the surface chemistry of lithium metal (chemical composition) upon contact with polymer electrolyte. Fig. 9(a) shows the FTIR spectrum of sample (S9) and Fig. 9(b) and (c) obtained in situ from a thin lithium electrode (on a KBr window) in contact with PEO + $LiN(C_2F_5SO_2)_2$ and PEO + $LiN(C_2F_5SO_2)_2$ + chitin polymer membranes, respectively. A few new peaks have been obtained as indicated in Fig. 9(c). The surface chemistry of lithium electrodes in contact with NCPE revealed the formation of Li–O–C (1266 cm^{-1}) and LiN (483, 487 cm^{-1}) compounds. However, the formation of these compounds does not influence the increase in the interfacial resistance of the Li/NCPE/Li systems.

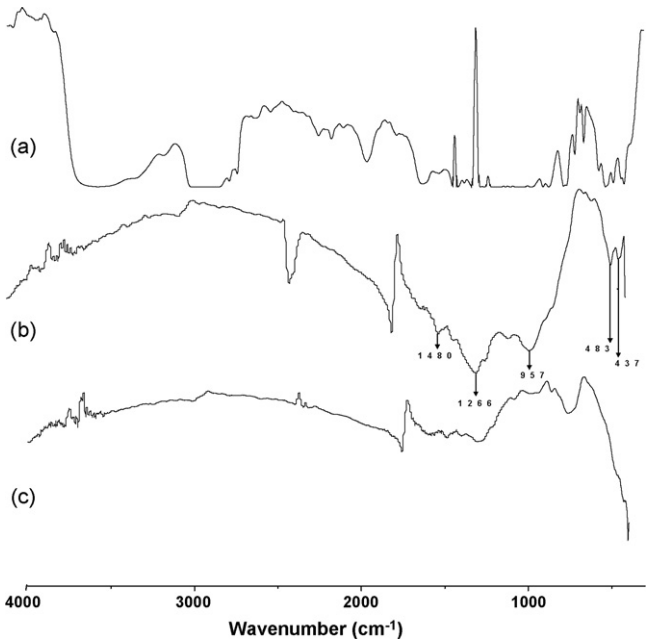

Fig. 9. FTIR spectrum of (a) sample S9; in situ from a lithium surface in contact with, (b) PEO + LiTFSI, and (c) PEO + chitin + LiTFSI.

3.6. Cycling studies on Li/NCPE/$LiFePO_4$ cells

The cycling profile of the Li/$LiFePO_4$ polymer cells was investigated as a function of temperature at C/10-rate. Fig. 10 shows the voltage/time profile of the first charge–discharge cycle obtained at 60, 70 and 80 °C. The polymer cell is capable of maintaining the same voltage almost during the entire discharge process which is a pre-requisite of a polymer battery system. Among the three temperatures studied, the system cycled at 80 °C indicates better behavior of the Li/$LiFePO_4$ polymer cell. An apparent change in the plateau was observed at 60 and 70 °C. This change is attributed to the following factors namely increase of the ionic resistance of the PEO electrolyte membrane, diffusive properties, a decrease of the electronic conductivity of the $LiFePO_4$ active material and the increase of the charge transfer resistance at the NCPE/$LiFePO_4$ composite cathode interface [23]. These results are in accordance with Appetecchi et al. [23] where the authors reported the cycling behavior of PEO–$LiCF_3SO_3$-based electrolytes at different temperatures and at current densities. However the authors achieved a maximum discharge capacity of 140 mAh g^{-1} at 100 °C. In the present study the cycling studies have been performed below 80 °C. The cycling behavior of Li/$LiFePO_4$ with NCPE at different temperatures and at different current densities is under progress and will be communicated in future.

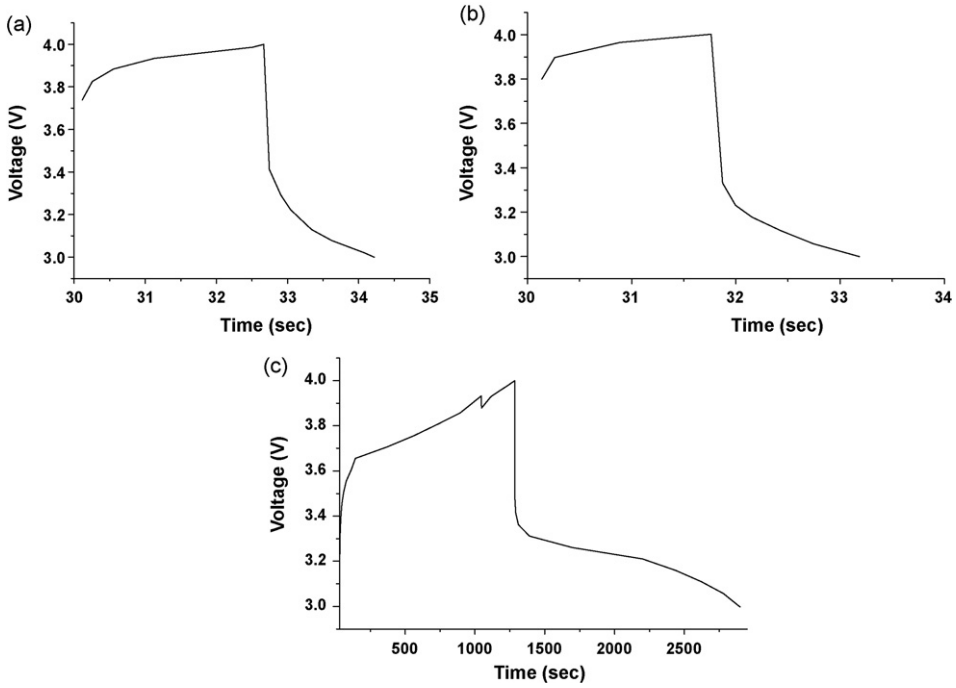

Fig. 10. Cycling performance of Li/NCPE (sample S5)/$LiFePO_4$ cells at C/10 rate.

4. Conclusions

PEO-based nanocomposite electrolytes with different compositions of chitin and LiBETI were prepared by a hot press method. The ionic conductivity increases with the increase of both chitin and LiBETI salt concentrations. Thermal analysis shows that PEO/chitin/LiBETI electrolytes are thermally stable up to 170 °C. The value of interfacial resistance "Ri", has been found to be lower for chitin-added sample than that of filler-free sample under open circuit conditions at 80 °C. Surface chemistry studies revealed the formation of new compounds on lithium surface which, however do not make any significant impact on the interfacial resistance of the Li/NCPE/Li system. The cycling behavior of Li/$LiFePO_4$ with NCPE at different temperatures and at different current densities will be communicated in near future.

References

[1] J.M. Tarascon, M. Armand, Nature 414 (2001) 359.
[2] F. Croce, G.B. Appetecchi, L. Persi, B. Scrosati, Nature 394 (1998) 456.
[3] P.G. Bruce, Solid State Sci. 7 (2005) 1456.
[4] A. Abouimrone, I.J. Davidson, J. Electrochem. Soc. 154 (2007) A1031.
[5] Y.G. Andrew, P.G. Bruce, Electrochim. Acta 45 (2000) 1417.
[6] P.G. Bruce, Electrochim. Acta 40 (1995) 2077.
[7] A.M. Christie, S.J. Lilley, E. Staunton, U.G. Andreev, P.G. Bruce, Nature 433 (2005) 50.
[8] A. Manuel Stephan, Eur. Polym. J. 41 (2006) 21.
[9] A. Manuel Stephan, K.S. Nahm, Polymer 47 (2006) 5952.
[10] A. Manuel Stephan, S. Gopu Kumar, M.A. Kulandainathan, N.G. Renganathan, Eur. Polym. J. 41 (2005) 15.
[11] G.B. Appetecchi, F. Croce, B. Scrosati, Electrochim. Acta 40 (1995) 991.
[12] H.J. Rhoo, H.T. Kim, J.K. Park, T.S. Huang, Electrochim. Acta 42 (1997) 1571.
[13] E. Quartarone, P. Mustarelli, A. Magistris, Solid State Ionics 110 (1998) 1.
[14] E. Peled, D. Golodnitsky, G. Ardel, V. Eshkenazy, Electrochim. Acta 40 (1995) 2197.
[15] F. Croce, R. Curini, A. Martinello, L. Perci, F. Ronci, B. Scrosati, R. Caminiti, J. Phys. Chem. 103 (1999) 10632.
[16] W. Wieczorek, K. Such, J. Plocharrski, H. Wycislik, Solid State Ionics 36 (1989) 255.
[17] J. Weston, B.C.H. Steele, Solid State Ionics 7 (1982) 81.
[18] M. Rinaudo, Prog. Polym. Sci. 31 (2006) 603.
[19] K.G. Nair, A. Dufresne, Biomacromolecules 4 (2003) 1835.
[20] K.G. Nair, A. Dufresne, Biomacromolecules 4 (2003) 657.
[21] K.G. Nair, A. Dufresne, Biomacromolecules 4 (2003) 666.
[22] J.H. Shin, F. Alessandrini, S. Passerini, J. Electrochem. Soc. 152 (2005) A283.
[23] G.B. Appetecchi, J. Hassoun, B. Scrosati, F. Croce, F. Cassel, M. Solomon, J. Power Sources 124 (2003) 246.
[24] O. Chusid, Y. Gofer, D. Aurbach, M. Watanabe, T. Momma, T. Osaka, J. Power Sources 97–98 (2001) 632.
[25] L.Z. Fan, J. Maier, Electrochem. Commun. 8 (2006) 1753.
[26] R. Ribeiro, G.G. Silva, N.D.S. Mohallen, Electrochim. Acta 46 (2001) 1679.
[27] T. Shodai, B.B. Owens, M. Ostsuka, J. Yamaki, J. Electrochem. Soc. 141 (1994) 2978.
[28] P.P. Chu, M.J. Reddy, H.M. Kao, Solid State Ionics 156 (2003) 141.
[29] C.Y. Chiang, M.J. Reddy, P.P. Chu, Solid State Ionics 175 (2004) 631.
[30] V.M. De Costa, T.G. Fiske, L.B. Coleman, J. Chem. Phys. 101 (1994) 2746.
[31] F.G. Pearson, R.H. Marchessault, C.Y. Liang, J. Polym. Sci. 13 (1960) 101.
[32] W. Huang, R. Frech, Polymer 35 (1994) 235.
[33] R. Frech, J.P. Manning, Electrochim. Acta 37 (1992) 1499.
[34] S.J. Wen, T.J. Richradson, D.I. Ghantous, K.A. Striebel, P.N. Ross, E.J. Cains, J. Electroanal. Chem. 408 (1996) 113.
[35] C.D. Robitailla, D. Fauteaux, J. Electrochem. Soc. 133 (1986) 315.
[36] C. Capiglia, P. Mustarelli, E. Quartarone, C. Tomasi, A. Magistris, Solid State Ionics 118 (1999) 73.
[37] W. Wieczorek, Z. Florjancyk, J.R. Steven, Electrochim. Acta 40 (1995) 2251.
[38] J. Przluski, M. Siekierski, W. Wieczorek, Electrochim. Acta 40 (1995) 2101.
[39] F. Croce, L. Persi, B. Scrosati, F.S. Flory, E. Plitcha, M.A. Hendrikson, Electrochim. Acta 46 (2001) 2457.
[40] Q. Li, Y. Takeda, N. Imanishi, J. Yang, Y.K. Sun, J. Power Sources 97–98 (2001) 795.
[41] Q. Li, N. Imanashi, A. Hirano, Y. Takeda, O. Yamamoto, Solid State Ionics 159 (2003) 97.